Chapter 3
Bio-microelectromechanical Systems (BioMEMS) in Bio-sensing Applications-Fluorescence Detection Strategies

Luis Acosta-Soto and Samira Hosseini

3.1 Introduction

The phenomenon of light emission upon a molecule absorbing electromagnetic energy is called fluorescence (Li et al. 2019). Fluorescence sensing is based on the theory of the target analytes mediated fluorescence quenching ("turn-off") or fluorescence enhancement ("turn-on") (Zhang 2019). Fluorescence biosensors operate based on the measurement of the fluorescence intensity. BioMEMS biosensors are recognized for their portability, excellent sensitivity, rapid analysis, and outstanding selectivity and have been extensively applied for the detection of different biomarkers (Li et al. 2019; Zhang 2019). Fluorescence detection method after colorimetric is the most commonly used spectroscopic method compared to other optical sensing strategies. For data analysis, fluorescence measurements relies on a variety of parameters, including fluorescence intensity, anisotropy, lifetime, emission and excitation spectra, fluorescence decay, and quantum yield (Li et al. 2019).

Fluorescence biosensors can help researchers study and analyze complex chemical processes within cells by incorporation of specific substances into the host cells (Ali et al. 2017). In comparison to the colorimetric detection strategy, fluorescence detection offers higher capacity of anti-inference, and higher sensitivity (Zhang 2019). Fluorescence detection, however, suffers from certain shortcomings including bleaching, light sensitivity, and background noise in signal readout.

L. Acosta-Soto · S. Hosseini (✉)
School of Engineering and Sciences, Tecnologico de Monterrey, Monterrey, Mexico
e-mail: samira.hosseini@tec.mx

S. Hosseini et al., *BioMEMS*, Lecture Notes in Bioengineering,
https://doi.org/10.1007/978-981-15-6382-9_3

3.2 Fluorescence Detection Strategy

Fluorescence is the process of the emission of light by a molecule or material called fluorophore after initial electron excitation in a light-absorption process. After excitation, the fluorophore temporarily retains its activity; this period is called fluorescence lifetime. The fluorophore returns to its original state of energy from that of excited state and the fluorescence emission can be observed with lower energy than the excitation. The fluorescence lifetime depends on the fluorophore and its interactions with the environment (Lakowicz and Lakowicz 1999; Baldini 2009).

Fluorescence detection is a suitable strategy for the development of biosensors since several parameters of fluorescence emission can be measured and recorded. These include fluorescence intensity, fluorescence emission spectrum, fluorescence excitation spectrum, emission anisotropy, and fluorescence lifetime (Stenken 2009). These parameters can be determined as a function of excitation and emission wavelengths. They can be used to detect the presence of different biomarkers and therefore there is an increasing demand for fluorescent sensors with fast response, high sensitivity, high selectivity, portability, and ability to perform real-time analysis. The latest examples of fluorescent BioMEMS biosensors are discussed in Table 3.1.

3.3 Recent Advances of Fluorescence Detection in Paper-Based BioMEMS

Biosensors based on fluorescence detection are designed and fabricated for a versatile class of platforms (Tiwari et al. 2017, 181–190). Paper-based biosensors offer certain challenges alongside and benefits when implementing fluorescence detection. Paper-based devices commonly rely on capillary forces to drive sample and reactants along a path traced for desired interactions. Moreover, these devices have the characteristic of being distinctly simple to operate, analyze, and dispose.

PADs have shown to have been extensively used as detection tools or as parts of more complex devices that may carry out multi-step processing pertaining the sample volume to the micro scale (Table 3.1) (Rosa et al. 2014; Zhang et al. 2015; Sonobe 2019)). As it was mentioned, μPAD operate based upon the capillary forces, offering cost-effective replacements for plastic and glass materials that are typically used for microfabrication. Through capillary forces, the fluids can be directed towards a specific direction by modifying the paper with hydrophobic barriers and patterns that can prevent or allow flow of substrate in highly specific directions. Capillary forces have the potential to drive fluid in a targeted direction without the need for pumps, syringes, or even rotating platforms. Paper are also benefited from the geometry of interwoven fiber network that provide high surface area for enhanced affinity towards analytes, thus facilitating detection. The higher surface area of paper materials allows stronger detection signal and lower limit of detection (LOD). Some of the latest

Table 3.1 Recent BioMEMS platforms for fluorescent detection: Type of the platform, main components, fabrication strategy, mechanism of operation

BioMEMS platform	Main components	Fabrication strategy	Mechanisms of operation	Detected analyte	Specifics	Ref
μPAD	• ZnO-NRs • WFP	The paper device was fabricated by treating WFP with a standard hydrothermal process to grow ZnO-NRs. Using salinization chemistry, capture antibodies were bound to the surface of the treated paper	Functionalized paper was exposed to sample flow to promote analyte-surface interaction followed by exposure to HRP conjugated secondary antibodies for the final readout	Cardiac Myoglobin	The μPAD can be used both as a passive pre-concentrator and an analytical device itself	Tiwari et al. (2017)
	• WFP • CBM-ZZ • IgG-FITC	Micro-channels are wax printed onto the surface of the WFP and then melted. WFP was exposed to CBM-ZZ. IgG-FITC was deposited on to the paper for subsequent detection	The analyte sample was directed in the paper by capillary forces through different analysis stages for biorecognition	Biotinylated-DNA	The final test performed showed little to no detection of analyte despite its known presence, leaving room for improvement of the device	Rosa et al. (2014)

(continued)

Table 3.1 (continued)

BioMEMS platform	Main components	Fabrication strategy	Mechanisms of operation	Detected analyte	Specifics	Ref
	• WFP • $TbCl_3$	The channels and corresponding grading scale were printed onto paper. Later, $TbCl_3$ was deposited on top of the paper to be absorbed	The tear samples were deposited onto the device, and after pre-defined lapse of time the device was tested for fluorescent signals for quantification of lactoferrin concentration	Lactoferrin	An antibody-free method for detection of lactoferrin in tear fluid was experimentally validated	Sonobe (2019)
	• WFP • Geometric radial pattern	The pattern was designed via graphic-design software, and later was wax printed onto WFP using a heating/melting mechanism	Sample was deposited into center port and traveled across the platform by capillary forces towards the analytical zones	• Ag • Hg • Aminoglycans of antibiotics	Though intended to interact with only one antibiotic, the similarity between different antibiotics from this family allows detection of multiple analytes of interest	Zhang et al. (2015)

(continued)

Table 3.1 (continued)

BioMEMS platform	Main components	Fabrication strategy	Mechanisms of operation	Detected analyte	Specifics	Ref
OLED hybrid integrated polymer microfluidic biosensor	• OLED • PDMS microfluidic chip • Inlets and outlets • Rinsing ports	Pre-PDMS was prepared by curing agent prior to casting over metal master-mold, which was later cured in an oven at 90 °C, and then bound to a second PDMS sheet. Moreover, ITO was lithographically patterned and treated by oxygen plasma before being subjected to a vacuum chamber for organic material evaporation	In sterilized PDMS chip, fluids were guided by suction towards mixing chamber. General sandwich immunoassay was carried out to trap the analyte and tag it. To obtain a fluorescent response, the OLED was activated with a 9 V variable DC voltage source, and response was measured through a spectrometer	Donkey anti-sheep IgG	A minimum emission response was detected at a concentration 5 times lower than that of original sample (2 μg/mL) If properly sterilized with water and iso-propyl alcohol (IPA), the device can be used up to 3 times	Acharya et al. (2015)

(continued)

Table 3.1 (continued)

BioMEMS platform	Main components	Fabrication strategy	Mechanisms of operation	Detected analyte	Specifics	Ref
3D microfluidic device with embedded micro-ball lenses array	• 3D multilayer PDMS • Solid micro-ball lenses	A photolithography process was used to fabricate a SU-8 post array on a silicon wafer, which was used to cast PDMS microwells following a soft lithography protocol. Glass microspheres were spread on the surface of the well array and swept into them	A high-power laser diode provided fluorescence excitation on cells through a micro-ball lens array. Multicolor fluorescence emission from cells were collected by the same micro-lens array and imaged by a high-speed CMOS camera through telescope optics	Live Mammalian cells	The fluid flow should be centered in order to achieve optimal uniformity in signal detection	Fan et al. (2013)

(continued)

Table 3.1 (continued)

BioMEMS platform	Main components	Fabrication strategy	Mechanisms of operation	Detected analyte	Specifics	Ref
Lab-on-chip	• Monolith column • LIF system • Inlets	Hot embossing was used to transfer channel features into the propylene microdevices with the help of CNC aluminum masters, while the holes were drilled for inlets and outlets. The monoliths were formed by a single-step method by filling a device with polymerization mixture and photo initiator and exposing to UV light	A lysate sample was directed through the column monolith. The porous allowed selectivity to the target DNA. After a rinse step, captured DNA was released by heating the monolith above the melting point of the DNA	dsDNA from the carbapenemase gene	The lowest detected concentration of KPC amplicons was 100 pM using this LIF system. The capture efficiency of the target was 86%, while its labelling was done with 97% accuracy	Knob et al. (2018)

(continued)

Table 3.1 (continued)

BioMEMS platform	Main components	Fabrication strategy	Mechanisms of operation	Detected analyte	Specifics	Ref
	• CELL chips Oval-shaped chambers • CGG • Inlets • MIX chip	The chips were fabricated by soft-lithography and wet etching. Each resulting PDMS substrate was bonded to a glass surface by exposing the samples to air plasma	HeLa cells were cultured in 5 different CELL chips. The CELL chips are disconnected from the CGG chip to be placed within incubator. The MIX chip was connected to the CELL chip to let the probe solution interact with the cells	PS beads as model analyte	Proposed platform reduces the time necessary for the assay by ~40%	Montón et al. (2017)

(continued)

Table 3.1 (continued)

BioMEMS platform	Main components	Fabrication strategy	Mechanisms of operation	Detected analyte	Specifics	Ref
	• PDMS • Micro-spheres	The PDMS chip was fabricated through soft lithography bound to glass slides using a plasma cleaner. The polystyrene micro-spheres were exposed to streptavidin, and the resulting conjugates were bound to a primary antibody for initial entrapment of insulin or insulin analog	A sample of T1D patients' blood was taken and pumped through the inlet of the device. As the sample flows through the channel, it is intersected with functionalized micro-spheres and subsequently conjugated with secondary antibody fluorescently tagged. The mixture travelled through outlet channel to be imaged for the final readout	Insulin analogs	The device accurately detected the insulin levels within 30s of injecting sample into the chip	Cohen (2017)

(continued)

Table 3.1 (continued)

BioMEMS platform	Main components	Fabrication strategy	Mechanisms of operation	Detected analyte	Specifics	Ref
	• PDMS chip • Bacterial trap Poly-Si-photogate	Through soft lithography, the PDMS chip was made from SU-8 mold and subjected to oxygen plasma to bind to lid. Channel and chamber geometry were defined accordingly to accommodate the micro-beads. Si-photo sensor was placed directly below the chip	Bacteria solution was pumped into the chip along with microbeads that helped trapping them within the setup fluorescence detection. The sample was excited through a UV light source, which was turned off to allow the Si-photogate to detect the fluorescent signals	L. pneumophila cells	This method offered a highly sensitive and timely option to identify bacterial presence without the need for optical sensors of more complex equipment for detection	Onishi (2017)
Electro-mechanical sensor	• 3D printed case • Microcontroller • Circuitry • Sample loading port	A ready-to-use biosensor that integrates a microcontroller, and corresponding circuitry to control a LED for excitation	Prior to loading the analyte solution, the device was calibrated with known concentrations for efficiently estimating the biomass composition of unknown sample	• Chlorophyll A and B • Phycocyanin	The error rate of the device was rather high (2–16%)	Shin et al. (2018)

(continued)

Table 3.1 (continued)

BioMEMS platform	Main components	Fabrication strategy	Mechanisms of operation	Detected analyte	Specifics	Ref
Alternative BioMEMS	• Micro-bead • RhB • FITC	Micro-beads were first incubated in alcohol solution to cause swelling. RhB penetrated the network and stained the beads. The beads were washed in deionized water to close the pores. Finally, it was submerged in a saturated solution containing FITC for staining and imaging	Upon excitation, the two fluorophores emitted different responses, one dependent solely on temperature (rhB), and another both on temperature and pH (FITC). This difference was used to identify them	Amino-PS beads based on temperature and pH	Sensor offered a great accuracy at 0.1 °C and 0.2 pH	Liu et al. (2014)

(continued)

Table 3.1 (continued)

BioMEMS platform	Main components	Fabrication strategy	Mechanisms of operation	Detected analyte	Specifics	Ref
	• Pt imprinted micro-motor • PC film • Pt • Ni	A PC film were Pt-deposited which was followed by coating with Ni, and a final layer of Pt. The surface of the cone-like structures which were integrated within the PC film was magnetically imprinted with phycocyanin molecules to leave exposed sites for binding	The device was placed in sea water. A combustible for propulsion was administered to the medium to initiate the motor's motion. The device can was guided with magnets in desired directions and was intentionally left in the sample prior to readout	Phycocyanin	This study offers a novel method for biorecognition that relies on magnetic force for locating the device	Zhang et al. (2013)

(continued)

Table 3.1 (continued)

BioMEMS platform	Main components	Fabrication strategy	Mechanisms of operation	Detected analyte	Specifics	Ref
	• Functionalized QDs • Organic quencher (BHQ2)	The QDs were conjugated to DNA strands designed to bind to analyte of interest	The sample was prepared by exposure to the analyte marker. In the presence of the analyte is present, will interact with the QD and quench the fluorescent signal. The mechanism of operation was based on Förster resonance energy transfer (FRET)	• DNA • MicroRNA	The DNA-QDs is benefited with excellent optical properties of QDs while using tailored properties of DNA for detection hence act as nano-sensors for nucleic acid detection	Su et al.(2014)
	• AuNC • FITC • PBS	AuNC was exposed to PBS to form PBA-AuNC. FITC was conjugated to this coupling complex and FA was subsequently incorporated to improve cellular membrane permeability	The complex of FA-FITC-BSA-AuNC demonstrates a high affinity towards the folate acceptor proteins on the cytoplasmic membranes of Hela cells. Once it has crossed the membrane, it can be used to monitor changes in pH as a function of the ratio of the stable AuNC emission in contract to that of FITC	Intracellular pH	The AuNC is highly permeable to the cytoplasmic membrane of cancerous cells	Ding and Tian (2014)

(continued)

Table 3.1 (continued)

BioMEMS platform	Main components	Fabrication strategy	Mechanisms of operation	Detected analyte	Specifics	Ref
	• Perceval sensor • PCR	The strategy for development of PercevalHR was based upon mutating the original Perceval sensor around the GlnK nucleotide-binding site	Relative concentrations of ATP to ADP within cells was used to monitor the metabolic activity of cells. Once the molecule has permeated the cytoplasmic membrane, fluorometric response to different excitation levels were monitored to determine the ATP:ADP ratio	Metabolic activity of cells	Although it brings a significant improvement in detection range over the first iteration, it still falls short of the total range that can be found within cells	Tantama et al. (2013)

The analyte of interest, and the advantages and disadvantages of each platform are presented in this table
Annexin V (Ann-V); Camptothecin (CAMPT); Computer numerical control (CNC); Direct current (DC); Double-strand DNA (dsDNA); Concentration gradient generating chip (CGG); Fluorescein isothiocyanate (FITC); Idium tin oxide (ITO); Immuno-globulin G (IgG); Iso-propyl Alcohol (IPA); Lab on chip (LOC); Laser-Induced Fluorescence (LIF); Microfluidic paper based analytical device (μPAD); Organic electroluminescent diode (OLED); Phosphatidyl-serine (Ps); Polydimethylsiloxane (PDMS); Polycarbonate (PC); Polymerase chain reaction (PCR); Quantum dots (QD); Terbium (Tb); Type 1 diabetes (T1D); Whatman filter paper (WFP); Zinc oxide nano-rods (Zn-NRs)

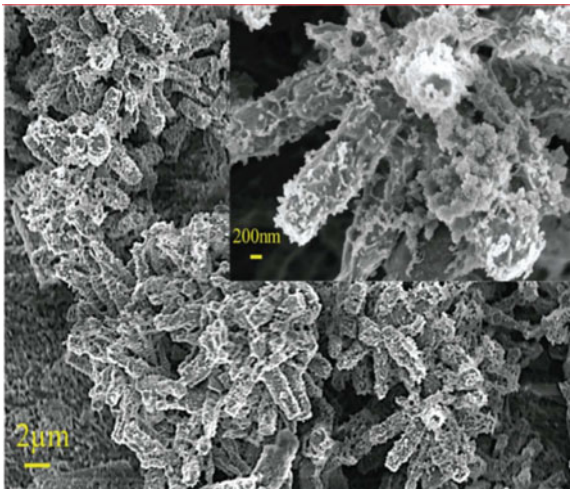

Fig. 3.1 WFP after functionalization; inset shows close-up of nano-rods after antibody immobilization (Tiwari et al. 2017)

examples of the paper-based BioMEMS used for fluorescence detection are provided in this chapter.

Tiwari et al. (2017) investigated the performance of Zinc oxide nanorods functionalized paper (ZnO-NRs-WFP) compared to regular Whatman filter paper (WFP) in the capture, detection, and release capabilities of the cardiac myoglobin. WFP was functionalized with nanorods (Fig. 3.1) that increased the surface area available to bind to the surface primary antibodies. With these paper alterations, the device showed a threefold improvement when compared to the control (non-functionalized) WFP. Although enzyme-linked immunosorbent assay (ELISA) protocol was used to demonstrate sensitivity and performance of the device through fluorescent detection of analyte posterior to exposure to secondary antibody, the results adduced the capability of molecular trapping, justifying future use as a preconcentration stage integrated into a multi-stage biosensor.

One of the main challenges of the paper materials for their use in biosensing is the fact that they commonly require functionalization to better interact with biomolecules. μPADs can be exposed to the biomolecules without functionalization as well (physical attachment). However, through many washing steps involved in bio-assays, these molecules may leach out of the fibrous structure of paper which expectedly results in undesirable detection outcomes. To avoid this, Rosa et al. (2014) investigated the use of the third family of carbohydrate binding module (CBM) of the *Clostridium Thermocellum*. This CBM has a high specificity towards cellulose and is therefore used as a part of a larger conjugate in order to bind the ZZ-domain of the staphylococcal protein A to the paper fibers. Once this interaction took place, the ZZ-domain from its free end can be used to bind to an IgG antibody. The IgG, in turn, can bind to and detect the presence of biotin. For that reason, if a DNA strand is biotinylated and fluorescently tagged, the presence of a fluorescent response in the paper would attest to the device's effectiveness in detection. The study demonstrated

that its mechanism of operation provides a reliable means for detection of analyte even though the signal was not comparable to that of EFP. This shortcoming was due to the lack of control over the orientation of fibers within the paper structure, resulting in unfavorable bonds with orientations that did not lend themselves to predetermined bindings hence dramatically decreasing the sensitivity of the device.

Dry eye disease (DED) is a condition that affects patients by causing complications in the production of lactoferrin, a chemical secreted in tears that protects the eye from an array of threats. This pathology is often diagnosed after a number of tests including ELISA. The μPAD proposed by Sonobe et al. (2019) operates on the basis of detection of lactoferrin in tear fluid. For fabrication of this device, WFP was embedded with terbium (Tb). Tb^{3+} reacts to lactoferrin and its conformation provides a fluorescent response to an excitation source. This response can be measured in terms of relative intensity, and, along with the linear design of the device, the height to which the column shows a fluorescent stain prior to excitation is indicative of the concentration of lactoferrin within the sample. Thus, an antibody-free method for detection of lactoferrin in tear fluid was proposed and experimentally validated (Sonobe 2019).

One of the main objectives of BioMEMS biosensors is to optimize the assay time. One of the methods for achieving a shorter analysis time is simultaneous screening of different analytes from a single sample. In the device proposed by Zhang et al. (2015) the simultaneous detection of three different contaminants in food was carried out. The geometry of the device allowed a central sample deposition from which the sample was guided towards several channels with already functionalized biomolecules targeted at different analytes. Figure 3.2 shows the scheme of the device. The surface of WFP was treated with graphene oxide, and the designed

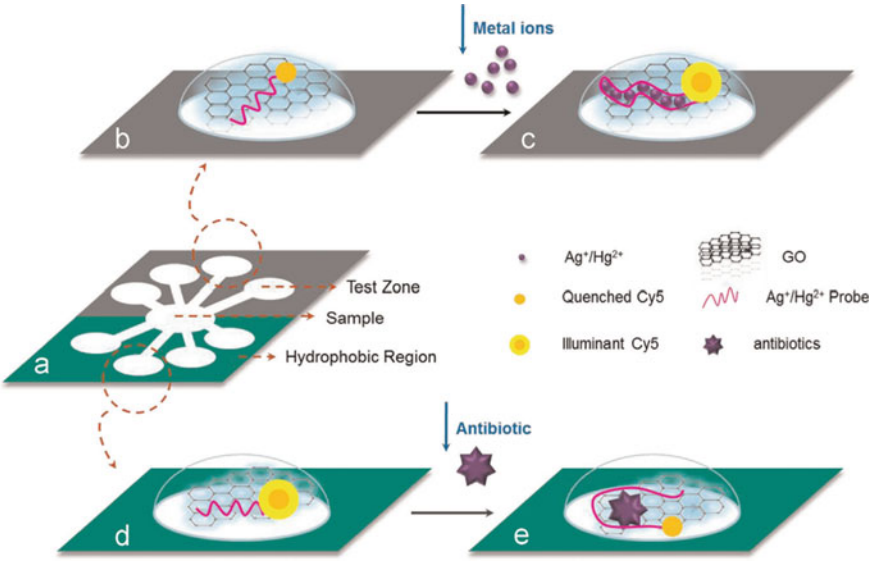

Fig. 3.2 Schematic of the final μPAD (Zhang et al. 2015)

geometry was created on the paper by wax printing. A half of the device was dedicated to the detection of metallic ions including Hg^{2+} and Ag^{+} via functionalization with ss-DNA strand that quenches the fluorescence of deposited Cy5 marker. Upon contact with the metallic ions, Hg^{2+} and Ag^{+} reacted with the thymine and cytosine bases respectively, which freed the Cy5 marker and allowed a fluorescent response to be read out. The second half of the device was devoted to the sensing of antibiotic residues. The method of detection in this other half was almost opposite as shown in Fig. 3.2. The interaction between the antibiotic residue and the graphene oxide surface, with the fluorescent probe, resulted in fluorescent quenching. Thus, the detection of this third analyte was measured by a decrease in the fluorescence signal. The device has shown a high level of specificity for the detection of the metal ions. However, it showed cross-compatibility between aminoglycoside antibiotics due to the similarly arranged amino groups that could react with the epoxy groups of the graphene oxide surface as well hence resulting in less reliable outcomes.

3.4 Microfluidic BioMEMS Recent Advances of Fluorescence Detection in Microfluidic BioMEMS

3.4.1 Recent Advances of Fluorescence Detection in Lab-On-Chip (LOC) Devices

Through the combination of biological assays such as ELISA with microfluidic technologies, it is possible to design biosensors that operate on minimal sample volumes and offer accurate detection outcomes, while being portable, and often reusable (Acharya et al. 2015; Fan et al. 2013; Knob et al. 2018; Montón et al. 2017; Onishi 2017). In this chapter some of the latest examples of the microfluidic BioMEMS for fluorescent detection are as provided.

The organic electroluminescent diode (OLED) has been studied as an economic and easy to manufacture source of light (energy). It is an attractive option not only for the possibility of reducing production costs, but also for the high degree of specificity it offers with respect to the light wavelength it emits. A device that integrates OLED in a microfluidic device was reported by Acharya et al. (2015). The proposed LOC (Fig. 3.3) used an AlQ3 OLED to activate fluorescent dye *Alexafluor 488* as part of a fluorescent assay for bio-optical detection of the antigens. The target antigen was anti-sheep IgGs, which were fluorescently tagged and were detected via a sandwich immunoassay after conjugating with monoclonal antibodies (Fig. 3.4). A common issue when designing such devices is the interference of the light source with the fluorescence as it may result in bleaching. To avoid such problem, a filter can be used to allow only certain wavelength of the emitted light to reach the sample and sensor. The excitation peak of the fluorophore should then be lower than the emission peak, thus allowing the tag's fluorescence to accurately reflect the presence of the antigen. Another concern regarding the OLED source is the inevitable heating of the

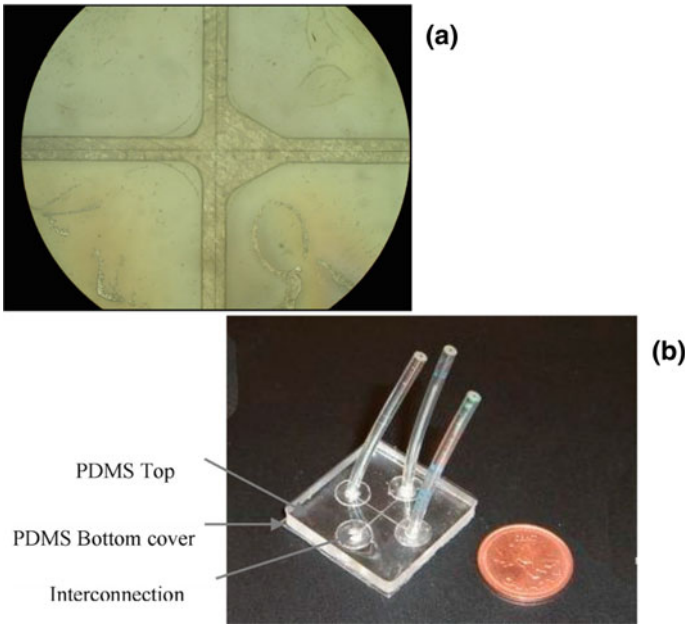

Fig. 3.3 Close-up of the device's chamber is shown on top (**a**); Below, the LOC from afar with the inlet an outlet channels labeled (**b**) (Acharya et al. 2015)

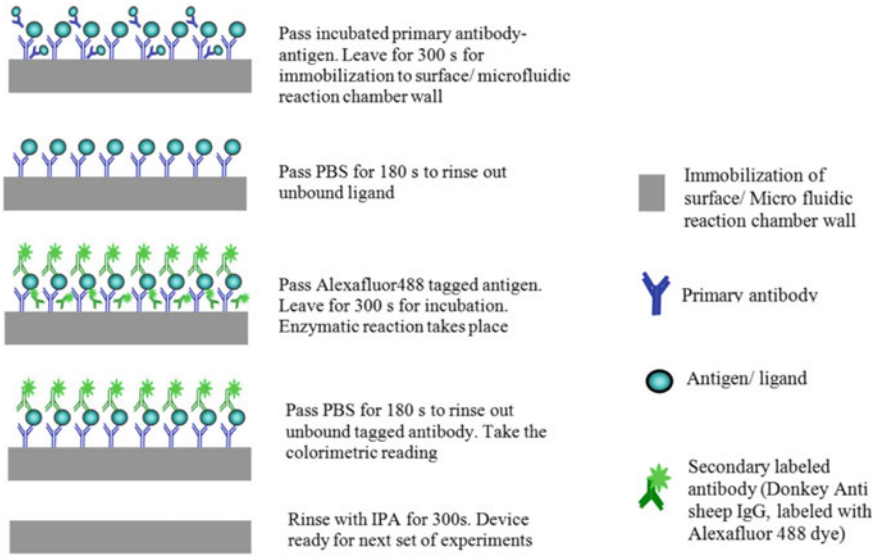

Fig. 3.4 An assay carried out for detection of anti-sheep IgG on AlQ3-OLED-LoC (Acharya et al. 2015)

components. To keep the effect of this increased temperature at negligible levels, the OLED was fed 9 V through a variable DC voltage source. Lower levels of LOD was achieved when the antibody was diluted 5 times the original concentration (2 μg/mL), that corresponded to a 1:1 ratio between the antigen and the secondary antibody. No relevant fluorescence was detected by the spectrometer after this point. The saturated sample with high concentration of biomolecules does not promote efficient binding between antigens and antibodies due to the possibility of steric repulsion. Despite the advantages of fluorescence-based biosensors utilizing an OLED, certain applications have design requirements that may place this as a suboptimal option.

In the case of multiple single sensing, various LOC configurations offered excellent platforms (Table 3.1). An example is a device that can screen up to 188,800 cells per second by profiling cells into 32 different channels (Fig. 3.5) that are simultaneously imaged (Fan et al. 2013). To achieve such high rate of imaging without the risk of false positive signal, the flow through the sample channels must be carefully focused. It was observed that the use of embedded micro-ball lenses (Fig. 3.5a) focused the analytes in the *x*–*y* plane at variable heights within the channel geometry. The spherical chromatic aberration of the lenses naturally magnified the fluorescent signals emitted by the assay, so long as the signal was aligned directly above the lens, which gave the LOC a high sensitivity. However, since the light entered the microball at once, if the procedure, for instance, demanded a cell to be tagged with two fluorophores, the colors would appear blended into a third tone on the final image. To separate the light into its original components, before reaching the camera lens, the light has traveled through a prism that refracted the emissions (Fig. 3.5b). By using

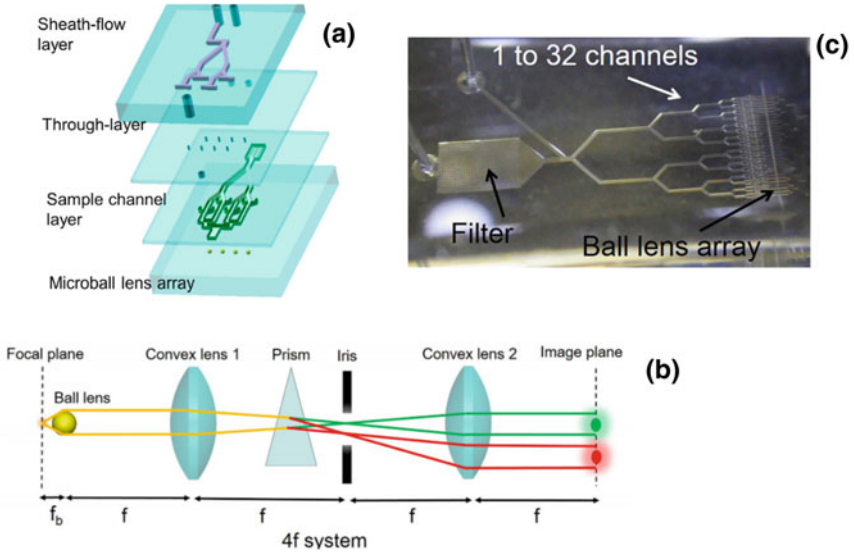

Fig. 3.5 **a** Shows the structure and build of the PDMS device **b** Portrays the fluorescence signal's trajectory **c** Shows final device (Fan et al. 2013)

this strategy, the device was tested with fluorescent dye *Lucifer yellow* in presence of the emission filter *Chroma 59,004* with transmission windows at both 500–535 nm and 570–620 nm resulting in satisfactory imaging and detection of the two windows. The smaller range corresponds to the green emission and the larger one to the red emission. An additional reason that this setup is a viable option for large-scale cells flow cytometry is the optimization of signal to the background and the source noise. The utilization of micro-ball lenses has improved this ratio 18 times against detection the systems without micro-ball lenses.

The objective of flow cytometry studies is usually to study live cells, rather than dyes. Fan et al. (2013) achieved detection of two cells (HeLa and Ramos cells) with different fluorescent tags along with accurate readout of respective proportions in the sample supplied to the device. Multiple and simultaneous imaging, however, is a demanding process, particularly when large volumes and fast results are needed. In any case, the sample must be initially tagged, which is not a simple task when the analyte is a strand of a genetic material.

One of the applications of LOC devices is the detection of antibiotic resistance in sepsis-related scenarios (Knob et al. 2018). In this case, specific DNA strands must be located and tagged for further analysis of a sample. This preparation requires the lysis of the sample bacteria cells, obtained through prior separation from the patient's cells. Once the genetic material is available, it is possible to employ various strategies to bind molecular markers to a given strand. Recently, a monolith within a polypropylene (PP) was used in a microfluidic device with specific functionalization to trap DNA sequences. In their study, Knob et al. (2018) immobilized genes related to Klebsiella pneumoniae carbapenemase (KPC). This was used as a mechanism to analyze the bacterial resistance to carbapenems by exposing extracted DNA to a monolith fabricated from crosslinkers exclusively. These crosslinkers were polyethylene-glycol diacrylate (PEGDA) and 3,4-Ethylenedioxy-N-methylamphetamine (MDMHA) functionalized with a tailored 90-mer specific to the DNA of interest. Once captured by the monolith, the genetic material was then exposed to hybridization probes designed as molecular beacons to bind the fluorophore to the target. For this step, the sequence needed to bind to the KPC genes was determined through software simulations and analysis. The study showed that a modified molecular beacon that has two fluorophores rather than just one was able to effectively detect and signal the presence of the target DNA. This has validated the use and functionality of the single-step fabricated monolith proposed for capture, labeling, and eluting of analyte.

Our understanding of the efficiency of molecular probes and dyes as fluorescent emitters has led the advancements in the field to another class of fluorophores, quantum dots (QD). QDs offer an alternative with higher photostability, availability, and adaptability for specific applications. QDs were applied in the detection of carcinoma cell apoptosis (Montón et al. 2017), as described in Table 3.1. When cells enter the state of apoptosis, it is common to observe the translocation of phosphatidylserine (Ps) from the inner layer of the cellular membrane to the exterior one. This presents a unique possibility to identify this process of cellular death by tracking Ps translocation through QD tagging. By binding a QD to the apoptotic cell, annexin V

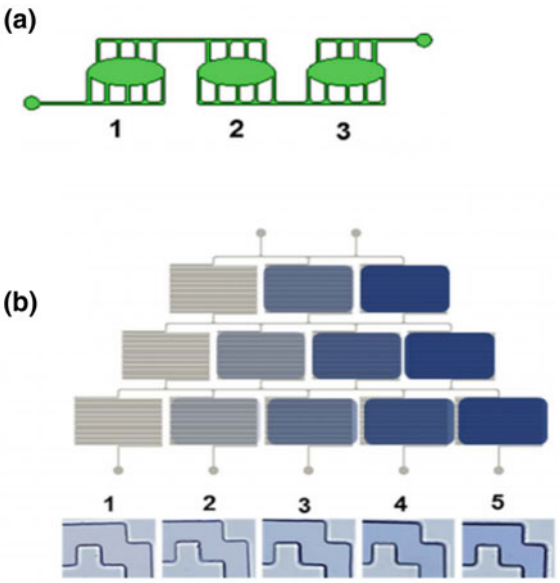

Fig. 3.6 **a** CELL chip **b** Concentration gradient generation chip exemplifying the 5 concentrations of CAMPT used by using a dye (Montón et al. 2017)

(Ann-V) can be conjugated to the QD. Ann-V has a high affinity towards Ps, acting as intermediary link between QDs and the apoptotic cells.

In the microfluidic device investigated by Montón et. al. (2017), two stages are proposed, each with their respective LOC, to cultivate, mark, and identify induction of apoptosis in cancer cells. The CELL chip proposed by the authors had different chambers for cell seeding (Fig. 3.6a). To achieve a monolayer on the CELL chip, samples were incubated for 24 h prior to exposure to camptothecin (CAMPT). Subsequently, the previously conjugated Ann-V-QD (in a separate PDMS device) was pumped into the CELL chip. This procedure was repeated for 5 different concentrations of CAMPT. The results showed a correlation between doses of the cancer treatment chemical and the Ann-V-QD labeled cells, establishing this device as a reliable tool for the bioassays. In the second design in order to induce cellular death, CAMPT was used again, however, it was diluted to a concentration gradient allowing the device to expose cancer cells to different CAMPT doses (Fig. 3.6b).

Modularity grants a high degree of adaptability to assays conducted within LOC devices at the cost of increased complexity. An approach to effectively implement multi-step assays inside a device was reported for determining insulin level and insulin-like factors in type 1 diabetes (T1D) patients (Cohen 2017). The proposed LOC relied on fluid mixing through the induction of transverse flow via serpentine geometries. The sample was introduced to the device via the inlet farthermost from the single outlet of the chip. The sample, once inside the device, was exposed to microspheres previously functionalized with antibodies specific to insulin and insulin-like factors. Taking advantage of the high surface area of spheres, exposure to analyte was magnified, reducing the time needed to achieve satisfactory mixing.

A secondary anti-insulin antibody conjugated with a fluorophore was then added to the system that signaled the presence of the analyte. The PDMS chip showed accurate readout of insulin in blood plasma within 30s without the need for washing of the secondary antibody. This allowed a continuous flow and real time detection within the device.

Although molecular tagging is typically used in fluorescence-based biosensors, some cells have a fluorescent response to UV exposure as well that can be used for detection purposes. In a device designed by Onishi et. al. (2017) the fluorescence of bacteria cells *L. pneumophila* was used to identify its presence within a sample. To trap the bacteria cells, they were mixed with micro-beads that helped form a barrier, or "stopper", that allowed concentration of bacteria cells to increase dramatically around the stopper. Once immobilized, the bacteria were exposed to UV radiation that provided a fluorescent response. This sensor enabled the detection of natural fluorescent bacteria without the need for optical or elaborate sensors and cameras.

3.5 Alternative BioMEMS for Fluorescence Detection

The feasibility of micro-beads as means to monitor changes in both pH and temperature was investigated by Liu et al. (2014). It was found that by using polystyrene (PS) micro-beads in combination with two different fluorescent markers (Rhodamine B and FITC) the fluorescent response of both fluorophores to an excitation source could be processed to obtain information about the medium in which they were submerged (Fig. 3.7). The PS micro-spheres were exposed to alcohol, causing them to swell thus via the open pores, Rhodamine B penetrated and stain the beads. To capture the Rhodamine B particles, the micro-beads were then rinsed in deionized water to shrink back the size hence closing the pores. Afterwards, the surface of the beads was stained with FITC. Since Rhodamine B and FITC have different excitation ranges, high wavelengths were used to elicit a fluorescent response. To demonstrate the detection mechanism, the microbeads were analyzed throughout ranges of both

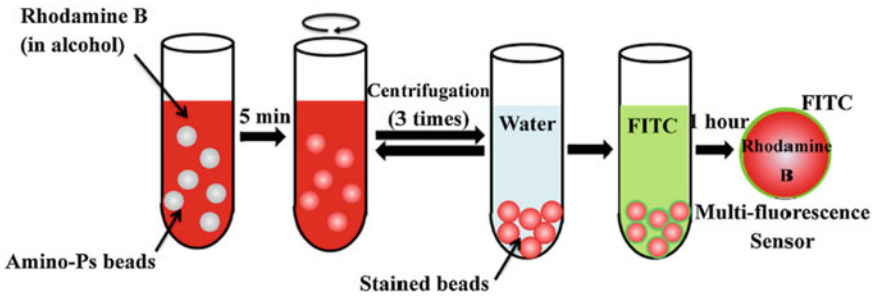

Fig. 3.7 Fabrication process of the micro-beads functionalized with Rhodamine B and FITC (Liu et al. 2014)

temperature (32–38 °C) and pH (5–8). Benefiting from the dependence of Rhodamine B's emission response on temperature, and the independence of it on pH levels, this compound was used for the calibration of the temperature within the medium. This information was then accounted for identifying the temperature dependence of the emission response generated by FITC, in order to accurately to identify the pH and its change in the experiment. The response to cyclic stimulation was observed to be remarkably consistent, as the beads gave the same response for a given configuration of the independent variables several times.

Zhang et al. (2013) reported a biosensor capable of selectively detecting, capturing, and transporting the analyte of interest, phycocyanin, which is closely related to the biomass of certain cyanobacteria (Fig. 3.8). This compound is a natural fluorophore acting as its own marker for detection and is commonly targeted for environmental applications. For fabrication process, a first layer of platinum (Pt) was deposited on a template membrane and then exposed to phycocyanin in an electric field that forced them through the membrane's pores and bound them to the outside of the cone-like structures (Fig. 3.8). Metal ions, Ni^{2+} and Pt^{4+}, were then electrochemically reduced from a solution into previously Pt-backed pores inside a template polycarbonate membrane. Once the air had been removed from the generated structures, the cone-like devices were modified with poly(3,4-ethylenedioxythiopene) (PEDOT)

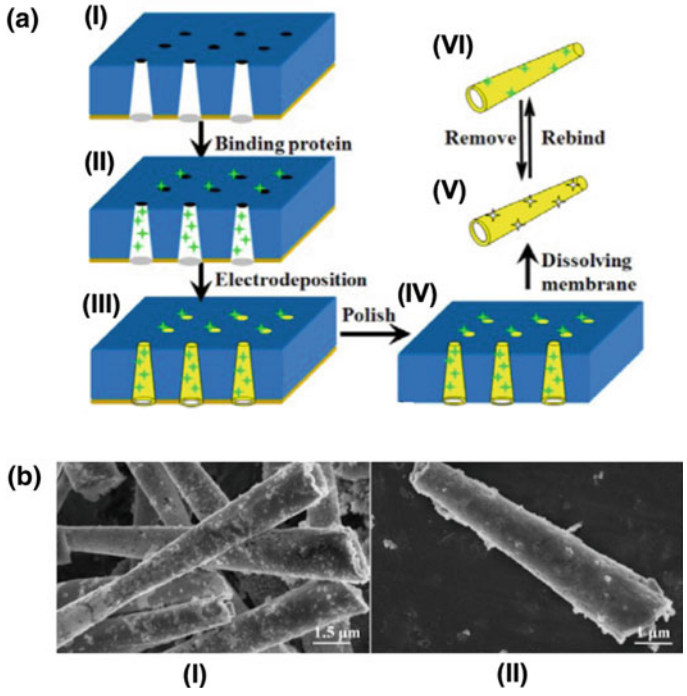

Fig. 3.8 **a** Elaboration of the magnetically imprinted biosensors. **b** Various (I) and single (II) magnetically imprinted cone-shaped sensors (Zhang et al. 2013)

layers that were electrochemically deposited onto the surface of the devices. Subsequently, a single Pt layer was galvanostatically deposited, to enhance the mechanical performance, followed by subsequent depositions of Pt-Ni, solely Ni, and finally Pt, in the same fashion (Fig. 3.8a). The template membrane was washed and sputter coated with gold. As a consequence, this fabrication strategy, the micro-motor was susceptible to magnetic fields, particularly when in accordance to its momentum. It was shown the micro-motor could be manipulated and guided towards specific areas when using sufficiently strong magnets. It is important to note, however, that control over micro-motor's motion depended on the geometry of the cone, as more asymmetrical structures will tend towards erratic spiraling paths given an uneven propulsion. The devices exhibited a targetable movement to target the phycocyanin. The earlier exposures of the cones left available binding sites on the outside surfaces of the cones (imprinted sites) that allowed a relatively quick adsorption of phycocyanin to the surface. Later evaluation in actual seawater showed that the presence of different molecules and compounds did not significantly interfere with the rate of phycocyanin adsorption or the movement and direction control of the micro-motors in the medium.

The detection of cyanobacteria (*Spirulina*) can be done using phycocyanin.

In specific cases, a need arises to simultaneously monitor the presence and ratio of several species within the same space. Such a scenario happens in biofuel production, where a specific ratio of green algae (*Chlorella vulgaris*) to cyanobacteria is desirable. Shin et al. (2018) took advantage of the fact that green algae produce chlorophyll a and chlorophyll b, both of which can produce a fluorescent response to the right stimuli. The proposed device is a ready-to-use biosensor that integrates a microcontroller, corresponding circuitry to control a LED used as excitation sources, along with an amplification circuit for the signal readout. The device is also equipped with a temperature compensating mechanism for the photodetector with an inlet for a vial with the sample to be analyzed and a screen that outputs the data from the test (Fig. 3.9). Unlike most fluorescent devices, this strategy heavily depended on the code that reads the sensors input. The code was responsible for the control and operation of the 3 LEDs that were used to obtain different responses from the three different fluorescent substances within the samples. Through the use of an amber LED, the response of phycocyanin was maximized, while for the two chlorophylls the signal was amplified. In the case of the blue LED, an UV source was used to measure total phytoplankton population, as it elicits similar responses from both *Spirulina* and *Chlorella vulgaris*. The algorithms used to process the information applied concepts of linear algebra analysis to correlate readouts of the three excitation sources and find relative concentrations of the different organisms. The partial least square regression (PLSR) method was used to best estimate the biomass of the different phytoplankton species. The device was calibrated by reading different samples with predetermined concentrations, and manually inserted into the microcontroller, before it can begin to quantitatively estimate unknown values. The device's predictions were within 2–16% of the real values of the respective biomasses. Reducing the background noise can further enhance the accuracy of prediction by this device.

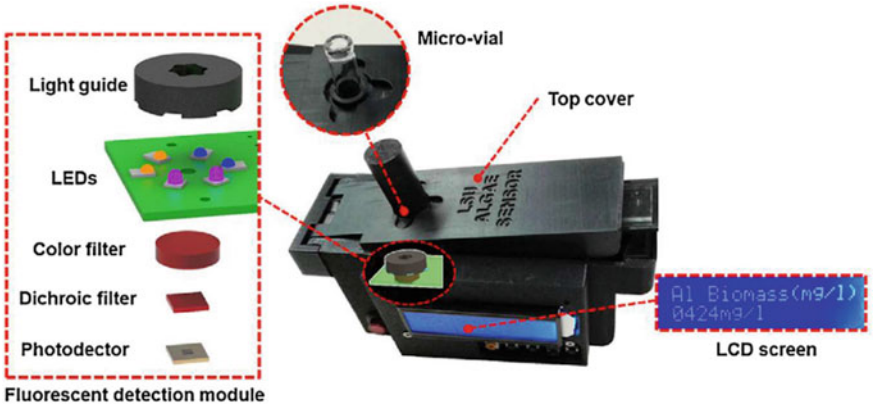

Fig. 3.9 Build of the multiple phytoplankton biosensor (Shin et al. 2018)

The identification of specific strands of genetic material including DNA or micro-RNA (miRNA) is of clinical importance to the detection and diagnostic of several pathologies. A new strategy for detection of such analytes with a high rate of specificity and selectivity was reported by Su et al. (2014). The method involved 3-mercaptopropionic acid (MPA)-capped QDs functionalized with thiolated DNA through ligand-exchange. The two reactants were mixed for several hours at different temperature ranges to achieve complete exchange between the two, resulting in DNA-QD conjugates. Förster resonance energy transfer (FRET) mechanism was used to ensure efficient energy transfer between the QD's and the BHQ_2-DNA (Fig. 3.10).

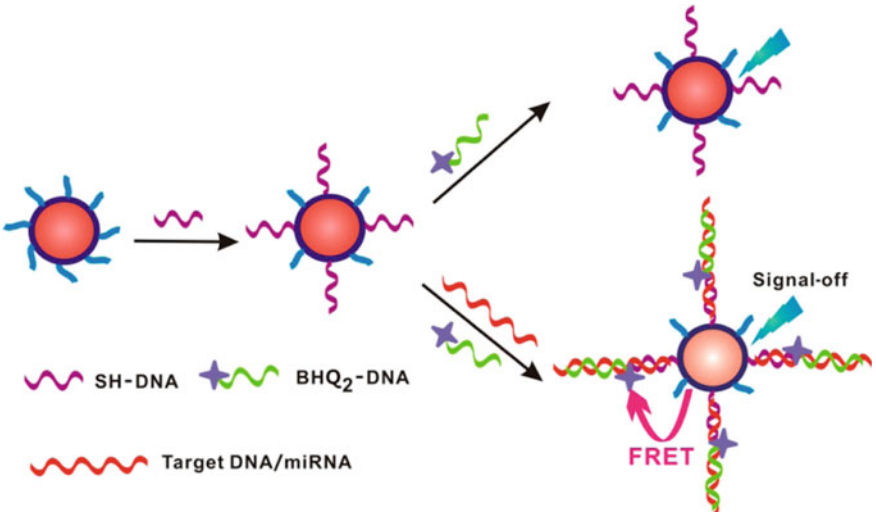

Fig. 3.10 Graphic visualization of FRET mechanism (Su et al. 2014)

The BHQ_2 served as an organic quencher that signals the acquisition of target sequence. The functionalized DNA-QD's exhibited a high degree of specificity in binding to target analyte, while avoiding interactions with other genetic sequences.

The previously alluded capability of FITC to tailor its fluorescent response to excitation depending on the pH of its medium was further investigated by Ding et al. (2014). Gold nano-clusters (AuNC) were encapsulated in bovine serum albumin (BSA) to protect the subjacent AuNC from the medium. The BSA-AuNC was stained FITC. Noteworthy, AuNCs emit a constant fluorescent response specific to its excitation wavelength, giving a static reference point that can be used to compare and calibrate the changes in the FITC response to the surrounding pH levels. Furthermore, the FITC-BSA-AuNC was exposed to folic acid (FA), creating a complex of FA-FITC-BSA-AuNC (Fig. 3.11), which had a high affinity towards the folate acceptor proteins on the cytoplasmic membranes of Hela cells. Due to the stability of the fluorescent response generated by AuNC (F_{AuNC}) at any pH, the ratio F_{FITC}/F_{AuNC} was used to determine the intracellular pH levels. The viability of this new sensor was tested in the presence of various ions typically found in the interior of complex living cells, including human cancer cells. The reported data supported the accuracy of the device, along with a short response time, indicating that treated AuNCs could be used for real time analysis of complex bioassays and biologic interactions.

Relative concentrations of ATP to ADP within cells represent a means to track the metabolic activity cells. Several attempts in fabrication of biosensors capable of crossing the cytoplasmic membrane and monitoring this ratio were made. Tantama et al. (2013) proposed a new version of their previous biosensor Perceval, renamed

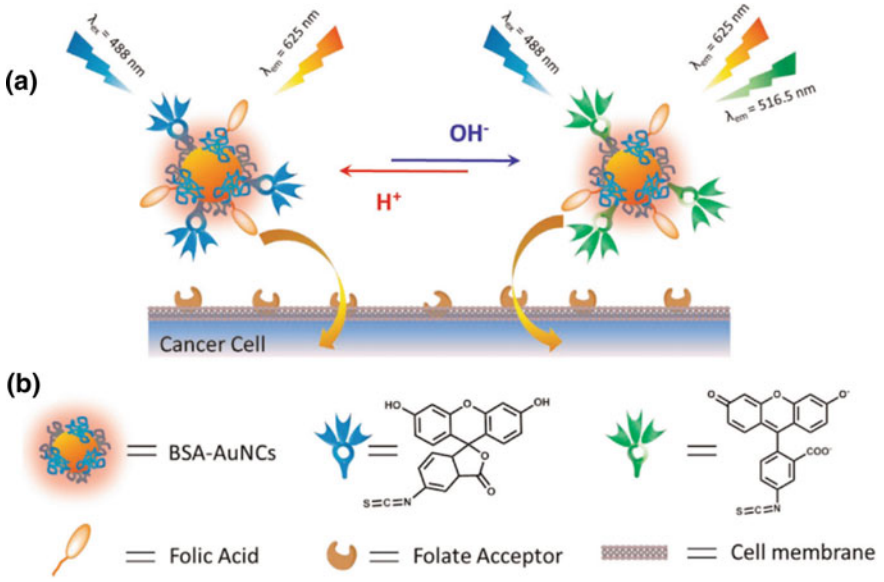

Fig. 3.11 Mechanism of operation of FA-FITC-BSA-AuNCs (Ding and Tian 2014)

as Perceval High Range (PercevalHR). The mechanism of operation in this biosensor relies on its affinity towards both ATP and ADP, while each reacts to different fluorescent wavelengths. ATP produces a fluorescent response for ~500 nm excitation, whereas ADP responds to ~420 nm. Through this difference, a ratio can be established for the relative difference between the responses recorded at one excitation or another, along with a third point (reference) at ~455 nm as an isosbestic fixed point. The biosensor was tested for neurons successfully. While adequate response was recorded to three different stimuli presented to disrupt regular metabolic rate of cells, the measured response was heterogeneous when tested for astrocytes. Such differences were minimized when pH bias was taken into consideration. The authors claimed to have recorded distinct responses for both ATP and ADP including the images recorded by two-photon microscopy. This method, in particular, opens a possibility for simultaneous screening of different metabolic activity within layers of a tissue.

3.6 Summary

Recent advances in biosensors based on fluorescent detection demonstrated that the field of BioMEMS holds great promise for portable and reliable devices capable of performing high throughput bio-assays. Recent studies point towards the versatility of fluorescence detection by employing different fluorophores depending on the materials and reactants involved aimed at optimizing the signal output. The mission of BioMEMS biosensors is to minimize the sample size, while reducing the time and expertise required to carry out these lifesaving assays. To this end, papers, as a class of material that lends an array of properties for integration in various biosensor platforms made one of the greatest candidates for fluorescence detection. Paper can be integrated into different designs of LOCs while it can individually serve as a device itself. Fluorescence detection strategy portrays a series of beneficial features including high sensitivity, and ease of readout. Nonetheless, the fluorescence may also suffer from background signal noise, bleaching, and cross talk effects that impose certain challenges on this widely applied technique (Ramon et al. 2017).

References

Acharya A, Packirisamy M, Izquierdo R (2015) OLED hybrid integrated polymer microfluidic biosensing for point of care testing. Micromachines 6(9):1406–1420. https://doi.org/10.3390/mi6091406

Ali J, Najeeb J, Asim Ali M, Farhan Aslam M, Raza A (2017) Biosensors: their fundamentals, designs, types and most recent impactful applications: a review. J Biosens Bioelectron 08(01). https://doi.org/10.4172/2155-6210.1000235

Baldini F (2009) Alexander P. Demchenko: introduction to fluorescence sensing. Anal Bioanal Chem395(5):1195

Cohen N et al (2017) Microsphere based continuous-flow immunoassay in a microfluidic device for determination of clinically relevant insulin levels. Microchim Acta 184(3):835–841. https://doi.org/10.1007/s00604-017-2072-z

Ding C, Tian Y (2014) Gold nanocluster-based fluorescence biosensor for targeted imaging in cancer cells and ratiometric determination of intracellular pH. Biosens Bioelectron 65:183–190. https://doi.org/10.1016/j.bios.2014.10.034

Fan YJ et al (2013) Three dimensional microfluidics with embedded microball lenses for parallel and high throughput multicolor fluorescence detection. Biomicrofluidics 7(4). https://doi.org/10.1063/1.4818944

Knob R et al (2018) Sequence-specific sepsis-related DNA capture and fluorescent labeling in monoliths prepared by single-step photopolymerization in microfluidic devices. J Chromatogr A 1562:12–18. https://doi.org/10.1016/j.chroma.2018.05.042

Lakowicz JR, Lakowicz JR (1999) "Introduction to Fluorescence", in *Principles of Fluorescence Spectroscopy*. Springer, US, pp 1–23

Liu H, Maruyama H, Masuda T, Honda A, Arai F (2014) Multi-fluorescent micro-sensor for accurate measurement of pH and temperature variations in micro-environments. Sensors Actuators B Chem 203:54–62. https://doi.org/10.1016/j.snb.2014.06.079

Li C, Wang Z, Wang L, Zhang C (2019) Biosensors for epigenetic biomarkers detection: A review. Biosens. Bioelectron. 144:111 695. https://doi.org/10.1016/j.bios.2019.111695

Li Z, Askim JR, Suslick KS (2019) The Optoelectronic Nose: Colorimetric and Fluorometric Sensor Arrays. Chem. Rev. 119(1):231–292. https://doi.org/10.1021/acs.chemrev.8b00226

Montón H, Medina-Sánchez M, Soler JA, Chałupniak A, Nogués C, Merkoçi A (2017) Rapid on-chip apoptosis assay on human carcinoma cells based on annexin-V/quantum dot probes. Biosens Bioelectron 94:408–414. https://doi.org/10.1016/j.bios.2017.03.034

Onishi S et al (2017) Detection of bacterial fluorescence by the combination of MEMS microfluidic chip and si photodetector toward on-chip biological sensing. ECS Trans. 80(4):157–164. https://doi.org/10.1149/08004.0157ecst

Ramon C, Temiz Y, Delamarche E (2017) Chemiluminescence generation and detection in a capillary-driven microfluidic chip. Microfluid BioMEMS Med Microsyst XV 100(61): 100–610. https://doi.org/10.1117/12.2250765

Rosa AMM, Louro AF, Martins SAM, Inácio J, Azevedo AM, Prazeres DMF (2014) Capture and detection of DNA hybrids on paper via the anchoring of antibodies with fusions of carbohydrate binding modules and ZZ-domains. Anal. Chem. 86(9):4340–4347. https://doi.org/10.1021/ac5001288

Shin YH, Barnett JZ, Gutierrez-Wing MT, Rusch KA, Choi JW (2018) A hand-held fluorescent sensor platform for selectively estimating green algae and cyanobacteria biomass. Sensors Actuators B Chem 262:938–946. https://doi.org/10.1016/j.snb.2018.02.045

Sonobe H et al (2019) A novel and innovative paper-based analytical device for assessing tear lactoferrin of dry eye patients. Ocul Surf 17(1):160–166. https://doi.org/10.1016/j.jtos.2018.11.001

Stenken JA (2009) Introduction to fluorescence sensing introduction to fluorescence sensing. J Am Chem Soc 131(30)P10791–10791. https://doi.org/10.1021/ja903152j. (By Alexander P. Demchenko (National Academy of Science of Ukraine, Kiev). Springer Science + Business Media B. V.: www.springer.com. 2009. xxvi + 586 pp. $149.00. ISBN 978–1–4020–9002–8)

Su S et al (2014) DNA-conjugated quantum dot nanoprobe for high-sensitivity fluorescent detection of DNA and micro-RNA. ACS Appl Mater Interfaces 6(2):1152–1157. https://doi.org/10.1021/am404811j

Tantama M, Martínez-François JR, Mongeon R, Yellen G (2013) Imaging energy status in live cells with a fluorescent biosensor of the intracellular ATP-to-ADP ratio. Nat Commun 4. https://doi.org/10.1038/ncomms3550

Tiwari S, Vinchurkar M, Rao VR, Garnier G (2017) Zinc oxide nanorods functionalized paper for protein preconcentration in biodiagnostics. Sci. Rep. 7:1–10. https://doi.org/10.1038/srep43905

Zhang X et al (2019) Recent advances in the construction of functionalized covalent organic frameworks and their applications to sensing. Biosens. Bioelectron. 145:111 699. https://doi.org/10.1016/j.bios.2019.111699

Zhang Z, Li J, Fu D, Chen L (2013) Magnetic molecularly imprinted microsensor for selective recognition and transport of fluorescent phycocyanin in seawater. 207890. https://doi.org/10.1039/b000000x

Zhang Y, Zuo P, Ye BC (2015) A low-cost and simple paper-based microfluidic device for simultaneous multiplex determination of different types of chemical contaminants in food. Biosens Bioelectron 68:14–19. https://doi.org/10.1016/j.bios.2014.12.042